Laser Flash Photolysis Investigations of Diffusion-Controlled Reactions in Supercritical Fluids

Christopher B. Roberts,† Jianwei Zhang,† Joan F. Brennecke,*,† and John E. Chateauneuf*,‡

Department of Chemical Engineering and Radiation Laboratory, University of Notre Dame, Notre Dame, Indiana 46556

Received: December 29, 1992; In Final Form: March 8, 1993

Laser flash photolysis has been used to investigate the triplet–triplet annihilation (TTA) process of benzophenone ($Ph_2C{=}O$) and the self-termination reaction of benzyl radical ($Ph\dot{C}H_2$) in supercritical CO_2 and ethane. Kinetic measurements were performed at various pressures above the critical pressure along two isotherms, one close to the critical temperature of the solutions (35 °C) and one further removed (50 °C). The second-order rate constants obtained indicate that each reaction occurs at the diffusion limit when spin statistical factors are considered. No evidence of enhanced cage effects due to supercritical solvent clustering about diffusive encounter pairs or enhanced solute/solute interactions were observed in these experiments. Additionally, the photocleavage of dibenzyl ketone and the rate constants for decarbonylation of phenylacetyl radical ($PhCH_2\dot{C}O$) have been examined under the above conditions and do not show any anomalous behavior or cage effects.

Introduction

It is now well established that the local density of a supercritical fluid (SCF) about a dilute solute may be significantly greater than the bulk density of the fluid.[1] Solvatochromic probes have been particularly successful in demonstrating that this effect of enhanced solvent–solute interaction, often termed "local density augmentation" or "solvent clustering", is most dramatic in the compressible and low-density subcritical regions of the fluid.[2] This phenomenon has also invoked the possibility of solvent cage effects occurring in SCFs that are enhanced beyond those experienced in normal liquids. Recently, two cases of anomalous behavior in SCFs have been reported that have been attributed to such clustering effects. Randolph and Carlier reported[3] enhanced bimolecular rate constants for Heisenberg spin-exchange between nitroxide free radicals in supercritical ethane. The results were explained in terms of increased collision times due to local density augmentation about the encounter pair. Bright and co-workers[4] have attributed a decrease in the emissive rate of decay of pyrene excimer in SC CO_2[4a] and C_2H_4[4b] to a protective sequestering of the excimer by solvent clusters.

In order to test the generality of such solvent behavior we have used laser flash photolysis (LFP) and time-resolved absorption to directly probe potential SC solvent clustering effects about diffusive encounter pairs. The T–T annihilation (TTA) process of triplet benzophenone (^3BP) and the free radical termination reaction of benzyl radical ($Ph\dot{C}H_2$) have been chosen for study since each process is known to proceed through pure diffusion-controlled bimolecular reactivity that adheres to simple diffusion models in normal liquids. Additionally, insights into the integrity of SC solvent cages have been obtained by investigation of the mechanism of decomposition of the benzyl radical precursor, dibenzyl ketone, which complements the recently reported product studies[5] of substituted dibenzyl ketones in SCFs.

Experimental Section

Materials. Benzophenone (Aldrich, Gold Label) was used as received. 1,3-Diphenylacetone (dibenzyl ketone) (Aldrich, 99%) was further purified by multiple chromatographies (silica gel column; 50% CH_2Cl_2/hexanes). Carbon dioxide (Scott Specialty Gases, SFC grade) was used as received. Ethane (Scott Specialty Gases, Ultra High purity grade, 99.9% or Linde, CP Grade) was sequentially passed through an Alltech high-pressure oxy-trap and multiple high-pressure (Alltech) charcoal traps. All liquid solvents were Fisher, ACS certified and used as received.

Method. The high-pressure apparatus, the sample preparation, and the application of LFP to SCF samples have recently been described in detail.[6,7] Briefly, LFP experiments were performed using laser excitation perpendicular to a pulsed 1000-W xenon lamp monitoring source. Transient absorption signals were digitized with a Tektronix 7912 AD digitizer and a VAX-11/780 computer was used for experimental control and computer analysis. Laser excitation was provided from either a Quanta Ray DCR-1 Nd:YAG (266 or 355 nm; ~10 mJ; pulse width ~6 ns) laser system or a Lambda Physik EMG 101 MCS excimer laser operated at 308 nm (XeCl) (4–100 mJ; pulse width 10 ns). The choice of laser excitation and excitation conditions depended on the individual experiment (vide infra). Cutoff filters were used at all wavelengths greater than 420 nm in both spectral and kinetic measurements to eliminate overtones.

The high-pressure sample cells used in these experiments possessed 3-mL capacity and were fitted with Suprasil quartz windows having mechanical seals composed of lead and graphite packing. In all experiments the laser excitation beam was attenuated to completely fill the 7 mm diameter window. The effective excitation path length of the high-pressure cell was verified to be 7 mm. This was done by measuring the second-order rate constant for ^3BP by LFP in thoroughly deoxygenated CH_3CN in the high-pressure optical cell at atmospheric pressure.

Sample preparation typically consisted of placing an appropriate amount of precursor into an optical cell in order to obtain a suitable optical density (OD) (0.2–0.8) of the precursor at the laser wavelength. The cell was evacuated and loaded with the desired fluid by use of an Isco Model 260D high-pressure syringe pump or an HIP Model 50-6-16 hand-operated pressure generator. The samples were brought to temperature and maintained at ±0.1 °C with an Omega (Model CN-6070 A) temperature controller equipped with a Watlow Firerod cartridge heater and a platinum resistance thermometer which made direct contact with the fluid. Pressure in the cell was monitored to ±0.24 bar with a Heise (Model 901A) pressure gauge. Experiments were performed along the 35.0 and the 50.0 °C isotherms either at constant mole fraction or constant molarity. Constant mole fraction experiments were performed from high to low pressure (density) by release of homogeneous solution. Constant molarity experiments were performed from low pressure (density) to high pressure (density) by addition of solvent. For future reference and perspective, solvent densities along the isotherms studied are

† Department of Chemical Engineering.
‡ Radiation Laboratory.

0022-3654/93/2097-5618$04.00/0

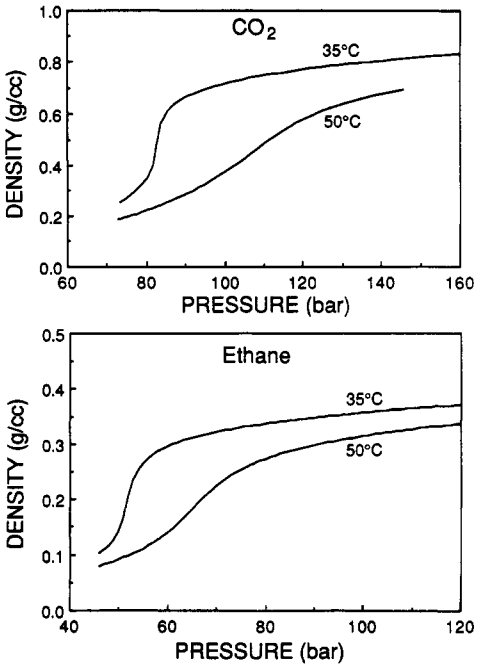

Figure 1. 35 and 50 °C isotherms for SC CO_2 (top) and ethane (bottom) densities.

presented in Figure 1 for both CO_2 (top) and ethane (bottom). The densities of CO_2 were calculated using the method of Angus et al. used to compile the IUPAC CO_2 density data,[8a] while ethane densities were calculated by a 32-term modified Benedict–Webb–Rubin equation of state.[8b] The critical pressure and temperature of CO_2 and ethane are (73.8 bar; 31.0 °C) and (48.7 bar; 32.2 °C), respectively.

Results and Discussion

Even though the transient species chosen for this study are chemically quite different, both reactions may be considered to occur in a bimolecular reaction in which diffusion of like species A + A occurs with a rate constant k_{diff} to form an encounter complex (AA) that may form product P with a rate constant k_P or diffuse apart at k_{-diff} according to eq 1. The experimentally

$$A + A \underset{k_{-diff}}{\overset{k_{diff}}{\rightleftharpoons}} (AA) \xrightarrow{k_P} P \tag{1}$$

observed rate constant for this process would then be

$$2k_{obs}^{AA} = \frac{k_{diff}k_P}{k_{-diff} + k_P} \tag{2}$$

and the reaction would be considered to be fully diffusion controlled, $2k_{obs}^{AA} = k_{diff}$, if $k_P \gg k_{-diff}$.

It has long been recognized, however, that for diffusion-controlled reactions there must be conservation of spin multiplicity. That is, products will *only* be formed from encounter complexes having similar multiplicities. Most ground-state reactions occur on the ground-state singlet surface throughout the reaction and are multiplicity-allowed processes. However, in the interaction of two triplets the encounter complexes formed have nine possible spin-states, and for the interaction of two doublet free radicals there are four. Since multiplicity must be conserved between the encounter complex and product, a spin statistical factor[9] (σ) must be accounted for in our experimentally observed rate constant, according to eq 3. The stoichiometry of the reactions being taken

$$2k_{obs}^{AA} = \sigma k_{diff} \tag{3}$$

into account, the spin statistical factor is $^5/_9$ for the disappearance of ^{3}BP and is $^1/_4$ for the termination of $PhCH_2$. Clearly, the factor is 1 for most ground-state reactions.

Experimentally, the second-order reactivity of both ^{3}BP[10] and $PhCH_2$[11] have been shown to be fully diffusion controlled in normal liquids and obey spin statistical factors. In the latter case, Fisher[11] has compared $PhCH_2$ reactivity in cyclohexane with k_{diff} calculated from diffusion coefficients of toluene as a model for $PhCH_2$. Excellent adherence to eq 3 was found, and $PhCH_2$ termination kinetics were suggested to be used for calibration purposes in studying diffusional processes.

1. Triplet–Triplet Annihilation of ^{3}BP. We have previously demonstrated that the spectral and temporal characteristics of ^{3}BP in pure CO_2 are very similar to those observed in CH_3CN solution.[6,7] There is no abnormal reactivity, complexation, or deactivation of ^{3}BP with CO_2. ^{3}BP generated from 355-nm LFP decays with clean second-order decay kinetics that are attributed to the annihilation process. Of course in order to obtain the true bimolecular rate constant ($2k_{TTA}$) the extinction coefficient (ϵ) of ^{3}BP is required according to eq 4

$$\Delta\left(\frac{1}{[A]}\right) = \frac{2k_{TTA}}{\epsilon l}t \tag{4}$$

where Δ[A] is the change in the ΔOD of ^{3}BP and l is the effective excitation path length. It was determined that ϵ of ^{3}BP in CO_2 was within 10% of that measured in CH_3CN[12] at 320 nm. Also, there is a <2% nonsystematic variance in ϵ in the pressure ranges studied. These determinations were made by comparisons of ^{3}BP OD in several LFP experiments in which all excitation conditions and ground-state BP absorbances were carefully matched in CO_2 and CH_3CN in the high-pressure cell at the appropriate pressures. Therefore, kinetics were measured at 320 nm and $2k_{TTA}$ was calculated using the previously determined[12] ϵ of ^{3}BP at 320 nm in CH_3CN of 11 500 M^{-1} cm^{-1}. In addition to determining that values of ϵ in CH_3CN and SC CO_2 were within the experimental and reported errors, the validity of the use of 11 500 M^{-1} cm^{-1} was tested by the calculation of $2k_{TTA}$ from the second-order decay measured in the LFP of BP in thoroughly deoxygenated CH_3CN in a standard 6-mm quartz cell. The value obtained $2k_{TTA} = 1.04 \times 10^{10}$ M^{-1} s^{-1}, using ϵ = 11 500 M^{-1} cm^{-1}, is equivalent to $^5/_9k_{diff} = 1.06 \times 10^{10}$ M^{-1} s^{-1} calculated from room temperature viscosity.[13]

In addition to $2k_{TTA}$ the rate expression (eq 5) for decay of ^{3}BP also contains k_1 for all unimolecular and pseudo-first-order deactivation processes. Therefore, decay kinetics were analyzed

$$\frac{-d[^3BP]}{dt} = k_1[^3BP] + 2k_{TTA}[^3BP]^2 \tag{5}$$

using an iterative technique[14] to determine the amount of first-order competition. Under laser excitation conditions in normal solvents k_1 is in the 1×10^5 s^{-1} range.[10b] In these experiments no significant first-order contribution could be detected. This analysis is particularly significant since we have previously measured[6,7] enhanced pseudo-first-order reactivity of ^{3}BP with added substrates in the compressible region of SCFs.

Also of great concern is the content of molecular oxygen present in the SCFs. We have previously demonstrated[7] that there was no measurable difference in the lifetime of ^{3}BP in the stock SFC grade CO_2 (rated at <2 ppm v/v) used and SFC grade CO_2 exposed to several freeze–pump–thaw cycles.

$2k_{TTA}$ in SC CO_2. The TTA process for ^{3}BP was studied in SC CO_2 at both 35 and 50 °C (Figure 2, top and bottom, respectively). Values of $2k_{TTA}$ ranged from 3.4×10^{10} to 1.4×10^{11} M^{-1} s^{-1} when measured at 35 °C in the 284–73 bar pressure range. The high-pressure point corresponds to near liquid like solvent densities of ca. 0.83 g/cm^3. The value of $2k_{TTA}$ increases slightly with a decrease in pressure and corresponding density

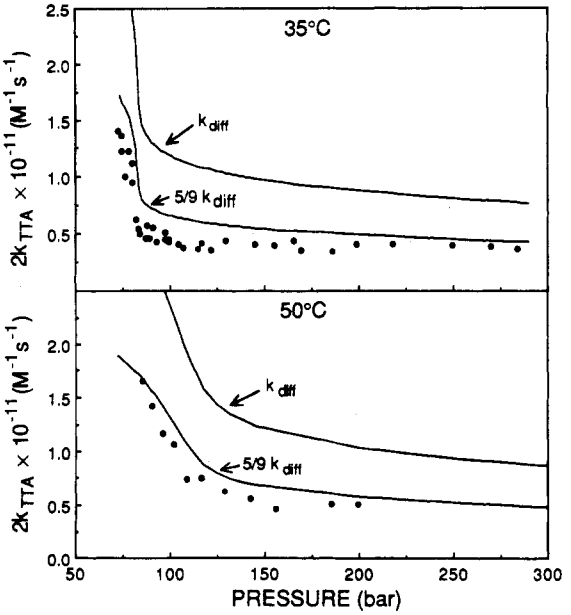

Figure 2. Pressure dependence of the TTA rate constant of ^{3}BP in SC CO_2 at 35 (top) and 50 °C (bottom) compared to respective k_{diff} values (see text).

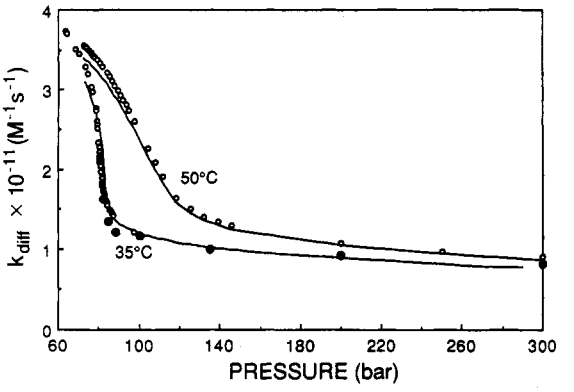

Figure 3. Values used to represent k_{diff} in SC CO_2 at 35 and 50 °C, calculated from the following: measured viscosities (o); calculated viscosities (—); and measured diffusion coefficients (●). See text, Methods 1, 2, and 3.

and then increases sharply below 100 bar with a decrease in pressure in the compressible region approaching the critical point. The low-pressure point corresponds to a dramatic drop in solvent density to ca. 0.25 g/cm^3. The error in $2k_{TTA}$ from the standard deviation of kinetic fits is only ca. 2%; however, the error associated with reproducibility ranged from ca. 5% in the high-density region to 10% in the medium density compressible region, and up to 20% in the highly compressible region near the critical pressure. These density region dependent errors were typical of all LFP experiments performed in this work and do not include errors in extinction coefficients.

The experimental data in Figure 2 are compared with k_{diff} and $^5/_9k_{diff}$. The values of k_{diff} at 35 °C were determined by three methods: (1) from previously measured viscosity data[15] and application of the Stokes–Einstein based standard Debye equation (SE/D), $k_{diff} = 8RT/3\eta$; (2) from viscosities calculated by the method of Thodos et al.,[16] which correlates dense gas viscosity to fluid density, and the SE/D equation; and (3) from measured diffusion coefficients[17] (D) for naphthalene as a model aromatic and the Smoluchowski equation, $k_{diff} = 4\pi N\rho D10^{-3}$, where N is Avogadro's number and ρ is the reaction distance. The individual data points determined from experimental quantities are in excellent agreement with the calculated values and are presented in Figure 3. It should be noted, however, that SCFs have been shown to deviate from hydrodynamic behavior and the use of

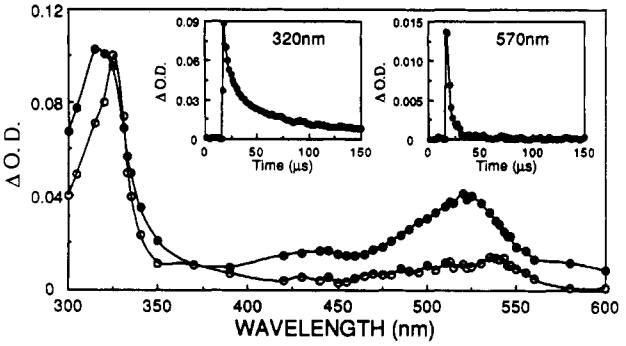

Figure 4. Transient absorption spectra monitored 2 (●) and 16 μs (O) after 355-nm LFP of benzophenone in SC ethane at 35 °C. Inserts: decay traces monitored at 320 and 570 nm.

Stokes–Einstein relationships to determine diffusion coefficients consistently results in overestimations.[18]

Figure 2 demonstrates that ^{3}BP $2k_{TTA}$ values fall well below the limit of diffusion in SC CO_2. In fact, $2k_{TTA}$ correlates very well with $^5/_9k_{diff}$ over the entire pressure range studied in total agreement with spin-statistical arguments.[9] The experimental values consistently fall slightly below the calculated $^5/_9k_{diff}$ curve, but it should be reemphasized that SE/D is known to overpredict k_{diff}. Figure 2 (bottom) demonstrates that $2k_{TTA}$ values measured further from the critical temperature, i.e., at 50 °C, also correlate well with $^5/_9k_{diff}$ calculated from viscosities determined by method 2 above.

LFP of Benzophenone in SC Ethane. Unfortunately, attempts to measure the TTA process of ^{3}BP in SC ethane were unsuccessful due to formation of a secondary transient species. The second transient was readily identified as benzophenone ketyl radical ($Ph_2\dot{C}OH$) by analysis of the time-resolved spectra and kinetics[19] presented in Figure 4. Unlike the CO_2 results, LFP in ethane resulted in wavelength-dependent decay kinetics. Monitoring at 320 nm, a species decaying with second-order kinetics over several tens of microseconds is observed (Figure 4, insert). Monitoring at 570 nm, where ^{3}BP but not ketyl radical absorbs, one observes a decay with pseudo-first-order kinetics with an observed rate constant (k_{obsd}) of 2.6×10^5 s^{-1} ($1/k_{obs} = 3.8$ μs). An absorption spectrum measured 2 μs following laser excitation represents a combined spectrum of both ^{3}BP and ketyl radical (Figure 4), while an absorption spectrum measured at 16 μs is solely due to ketyl radical as identified by its characteristic red shift[20] compared to ^{3}BP. Ketyl radical must be produced by ^{3}BP hydrogen-atom abstraction from a H-atom donor. Vigorous attempts to further purify the 99.9% ethane, or Linde CP Grade ethane, gave identical results to those observed in Figure 4. Therefore, we tentatively suggest that the hydrogen-atom source is the ethane itself, which initially is somewhat surprising considering that the bond dissociation energy of ethane is 100 kcal/mol.[21] However, ^{3}BP has been shown[22] to abstract primary hydrogen atoms from 2,2-dimethylpropane and 2,2,3,3-tetramethylbutane at 4.3 and 3.1 $\times 10^4$ M^{-1} s^{-1}, respectively, in CH_3CN at 25 °C. The molarity of pure ethane is 12.8 M at 35 °C and 140 bar.[8b] Therefore, assuming similar reactivity with ethane, the above bimolecular rate constants (k_{bi}) predict $k_{obs} = 4.0$–5.5×10^5 s^{-1} ($1/k_{obs} = 2.5$–1.8 μs) in pure ethane according to $k_{obs} = k_o + k_{bi}$[ethane] where k_o is the rate constant for decay of ^{3}BP in the absence of ethane.

2. Benzyl Radical Termination Reaction. *Benzyl Radical Absorption Spectrum.* Benzyl radical ($Ph\dot{C}H_2$) was generated by the photodecomposition of dibenzyl ketone (DBK).[11,23] Mechanistic details of the decomposition process of DBK in SCFs are discussed in the following section. The ground-state absorption spectrum of DBK demonstrated no spectral shifts in SC CO_2 or ethane compared to cyclohexane solution. For comparison with SCF experiments, $Ph\dot{C}H_2$ was generated by either 266- or 308-nm LFP of DBK in cyclohexane solution, resulting in the well-

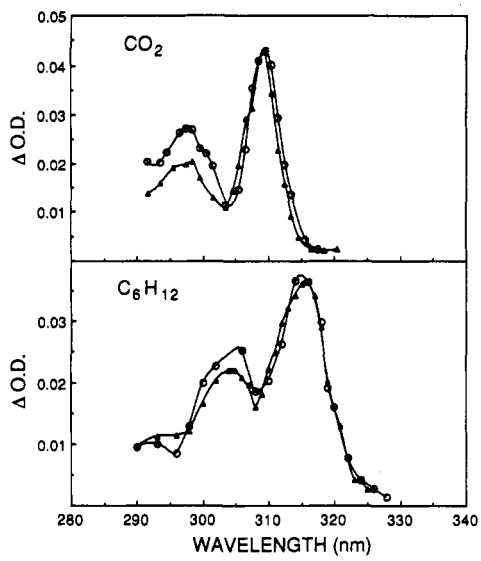

Figure 5. Top: Benzyl radical absorption spectra obtained in SC CO_2 at 35 °C at 134.7 (○) and 80.8 bar (▲). Bottom: Benzyl radical absorption spectra obtained in N_2-saturated cyclohexane at 141.4 bar (○) and atmosphere pressure (▲).

known absorption spectrum[24] of $PhCH_2$ possessing λ_{max} of the primary absorption band at 317 nm. Very little solvent effect is observed for either λ_{max} or ϵ of $PhCH_2$ in a variety of normal liquid solvents.[25,26] However, LFP of DBK in SC CO_2 resulted in an absorption spectrum of $PhCH_2$ having the primary absorption band shifted to 310 nm (Figure 5).

In order to determine if the observed spectral shift was a consequence of a "pure pressure effect" on the $PhCH_2$ transition, spectra of $PhCH_2$ were measured in pressurized cyclohexane. A comparison of $PhCH_2$ spectra measured in cyclohexane at atmospheric pressure and 141.4 bar are presented in Figure 5 (bottom). The spectra have been normalized to equivalent OD at 317 nm and demonstrate that no pressure-induced spectral shifts occur over the pressure range of interest to this study.

The effect of SC CO_2 solvent density on the absorption spectrum was also investigated. Only a slight (0.5–1 nm) spectral shift was observed (Figure 5, top) in the primary absorption band by varying solvent density (see Figure 1) from high pressure (134.7 bar) to low pressure (80.8 bar). Therefore, $PhCH_2$ demonstrates no significant solvatochromic behavior. Very similar results were observed in SC ethane where $PhCH_2$ also possessed a 310-nm maximum that only varied slightly with solvent density.

The origin of the spectral shifts observed in SC CO_2 and ethane becomes clear when the fluid phase spectra of $PhCH_2$ are compared to the spectrum in the vapor phase. Porter and Wright[27] reported the λ_{max} of the primary absorption band of $PhCH_2$ in the gas phase to occur at 305.3 nm. There is no significant pressure or solvent density effect on the shape of the $PhCH_2$ spectrum. Since CO_2 and ethane are nonpolar, one would expect that the spectral shift observed would be due primarily to London dispersion forces.[28] For dispersion forces only, one expects the bathochromic shift for a solute in solution compared to the isolated molecule to be proportional to a function f of the refractive index ($f = n^2-1/2n^2+1$). In fact, the absorption band of $PhCH_2$ in high-pressure SC CO_2 and ethane falls exactly as predicted between the vapor phase and aliphatic liquid hydrocarbons. The deviation from theory of the solvatochromic shift with change in pressure in supercritical fluids has been used to estimate local densities.[2] Actually, at lower pressures the benzyl radical shifts measured here are smaller than expected, which corroborates earlier findings[2] that the local density is greater than the bulk density at these conditions. However, the shift in the spectrum of $PhCH_2$ with pressure is sufficiently small that it is not a good probe of local densities.

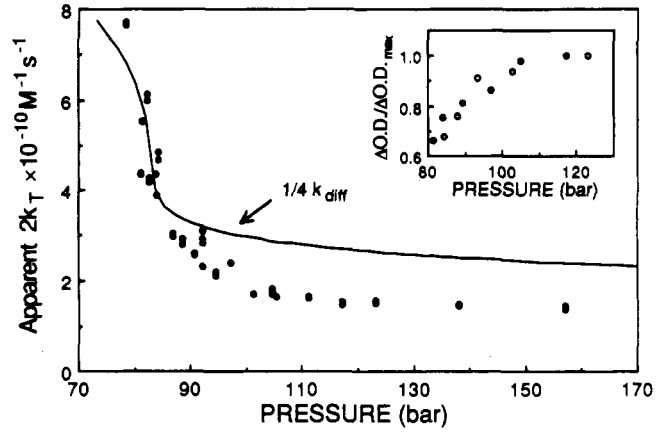

Figure 6. Uncorrected values of $2k_T$ for $PhCH_2$ (see text) versus pressure in SC CO_2 at 35 °C. Insert: Plot of $PhCH_2$ ϵ pressure dependence (see text) measured with 266 (•) and 308 nm (○) laser excitation.

$2k_T$ and ϵ of $PhCH_2$ in SC CO_2 and ethane. LFP (308 nm, 100 mJ) of DBK in thoroughly deoxygenated cyclohexane resulted in the measurement of clean second-order decay kinetics of $PhCH_2$ at 317 nm. An absolute rate constant for $PhCH_2$ termination ($2k_T$) of 4.75×10^9 M^{-1} s^{-1} was obtained using the ϵ of 8800 M^{-1} cm^{-1} previously determined by Fisher.[29] The value is in excellent agreement with that determined by Fisher in cyclohexane (4.9×10^9 M^{-1} s^{-1}) and values of $2k_T$ determined by several researchers using a variety of experimental techniques.[29]

Matched LFP experiments, similar to those described for benzophenone, were performed with DBK in SC CO_2 and cyclohexane. The ϵ of $PhCH_2$ in SC CO_2 at 35 °C and 114.6 bar was determined to be within 5% of the cyclohexane value. Therefore, in an initial experiment to measure the pressure dependence of $2k_T$ in SC CO_2 at 35 °C, the 8800 M^{-1} cm^{-1} value of ϵ was used. The experiment was performed at constant mole fraction of DBK. The results, presented in Figure 6, indicated that $2k_T$ exceeded the predicted $^1/_4k_{diff}$ value (calculated by method 2 as described above) at low density, in the compressible region, i.e., below 80 bar. However, a subsequent experiment performed at constant molarity of DBK quickly demonstrated that this observation was actually an artifact of a density-dependent ϵ of $PhCH_2$. The ϵ[30] of $PhCH_2$ rapidly decreased below 105 bar to ca. 65% of the high-pressure value. This is illustrated in Figure 6 (insert) and is presented as the ratio of the transient ΔOD of $PhCH_2$ measured at each pressure to the maximum ΔOD obtained at high pressure. Identical results were obtained using either 266- or 308-nm laser excitation. Similar results were observed for $PhCH_2$ in SC ethane, however, ϵ only decreased ca. 18% with decrease in pressure (density).

Therefore, to obtain true values for $2k_T$ for $PhCH_2$ the density-dependent changes in ϵ must be taken into account. Corrected values of $2k_T$ for $PhCH_2$ have been obtained in both SC CO_2 and ethane at 35 and 50 °C and are presented in Figure 7. Comparison of the experimental $2k_T$ values with the $^1/_4k_{diff}$ predicted values (method 2) indicates that $PhCH_2$ termination occurs near the spin-statistically-allowed diffusion-controlled limit in each solvent at all solvent densities studied. As before, the experimental values are slightly below the calculated values but the Stokes–Einstein/Debye equation consistently overpredicts k_{diff}, as mentioned above.[18]

3. DBK Photodecomposition and Decarbonylation of $PhCH_2CO$. The photodecomposition process of DBK was examined in some detail in SC CO_2 and ethane in order to determine the importance of SCF clustering on the individual decomposition events. The mechanism of decomposition of DBK in normal liquids has been well established[11,23] and occurs according to Scheme I. Photolysis of DBK results in rapid formation of triplet DBK following intersystem crossing (steps 1+2). Triplet DBK then undergoes

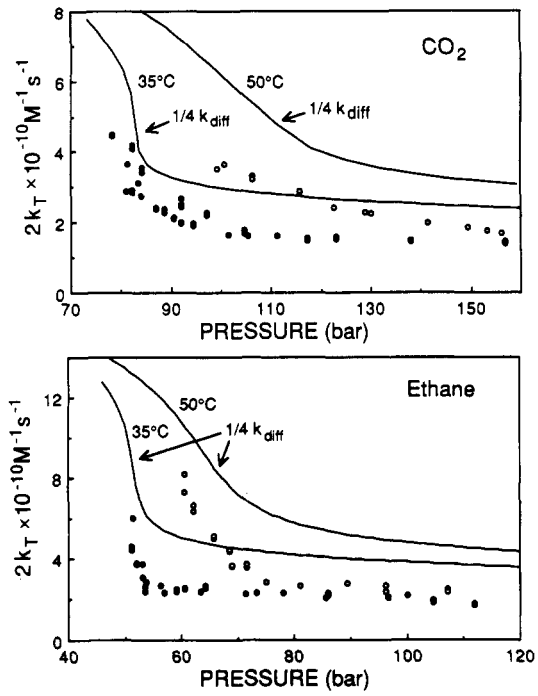

Figure 7. $2k_T$ for $PhC\dot{H}_2$ in SC CO_2 (top) and SC ethane (bottom) at 35 and 50 °C, compared to $^1/_4k_{diff}$ calculated from method 2 (see text).

SCHEME I

	Step
$(PhCH_2)_2C{=}O \xrightarrow{h\nu} (PhCH_2)_2C{=}O^{1*}$	1
$(PhCH_2)_2C{=}O^{1*} \xrightarrow{ISC} (PhCH_2)_2C{=}O^{3*}$	2
$(PhCH_2)_2C{=}O^{3*} \rightarrow Ph\dot{C}H_2 + PhCH_2\dot{C}{=}O$	3
$PhCH_2\dot{C}{=}O \xrightarrow{k_{-CO}} Ph\dot{C}H_2 + CO$	4
$2Ph\dot{C}H_2 \xrightarrow{2k_T} PhCH_2CH_2Ph$	5

type I homolytic cleavage to produce benzyl and phenylacetyl radical (step 3). Solution-phase LFP experiments have demonstrated[26] that this step occurs on the subnanosecond time scale. $PhCH_2\dot{C}O$ subsequently decarbonylates (step 4) with reported rate constants[31] of $k_{-CO} = 5\text{–}9 \times 10^6$ s^{-1} at room temperature. Then free $Ph\dot{C}H_2$ may undergo the termination process ($2k_T$) to primarily form bibenzyl product (step 5).

Of the individual steps outlined in Scheme I, steps 3–5 have the strongest potential to be influenced by SC cage effects. In the previous section we have clearly demonstrated that step 5 occurs with absolutely no inhibition or acceleration in SC CO_2 or ethane due to clustering effects. In order to determine the solvent influence on steps 3 and 4, one needs to analyze the individual absorption traces of $Ph\dot{C}H_2$ production measured on a relatively short time scale. As an example an absorption trace monitored at 310 nm observed upon 308-nm LFP of DBK in SC CO_2 at 35 °C and 104.7 bar is presented in Figure 8, insert. The result is similar to those observed in nanosecond LFP experiments of DBK in normal liquids,[31] where production of $Ph\dot{C}H_2$ is observed to occur in a two step mechanism. The instantaneous "jump" in the absorption trace coincides with homolytic cleavage step 3 and the first-order growth corresponds to the unimolecular decarbonylation step 4. The ratio of "jump" to growth, i.e., step 3 to step 4, was monitored with change in pressure and was found to remain constant. This indicates no change in the mechanism of step 3 with a change in solvent density. In other words, there is apparently no significant SC solvent cage effect on the geminate radical pair that would force in-cage radical–radical recombination. In normal nonviscous solvents, cage escape of the initial

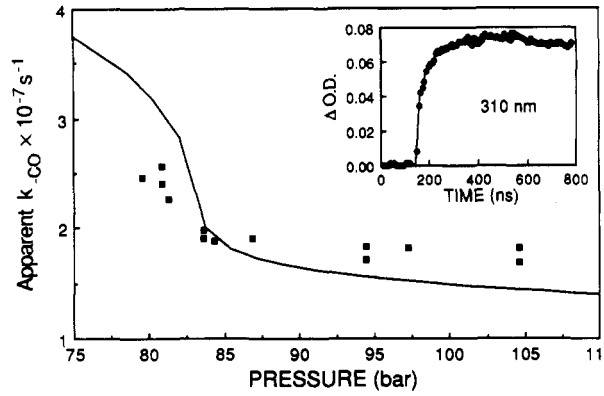

Figure 8. Apparent pressure dependence of k_{-CO} for $PhC\dot{H}_2CO$ in SC CO_2 at 35 °C. Insert: Typical absorption trace observed at 310 nm following LFP of DBK in SC CO_2 at 35 °C.

radical pairs formed in step 3 is >95%.[11] This result is in agreement with the recent report of Fox, Johnston, and co-workers[5] who found no change in the quantum yield of photodecomposition of nonsymmetrical substituted DBKs in SC CO_2 or ethane with change in solvent density.

The results of the pressure effect on the decarbonylation process (step 4) in SC CO_2 at 35 °C is also presented in Figure 8. k_{-CO} values were obtained from a first-order fit of the growth portion of the absorption traces and ranged from 1.7×10^7 s^{-1} at 104.6 bar to 2.6×10^7 s^{-1} at 80.9 bar. It is instructive to note that the modest 1.5 factor of increase in k_{-CO} occurs in the compressible region as demonstrated by comparison with the k_{diff} curve (Figure 8). We believe that the observed change in k_{-CO} is not actually due to a change in the decarbonylation rate constant but is an artifact of the competing decay $2k_T$ process which overlaps the absorption growth. The $2k_T$ process, of course, is faster in the compressible region. There is precedence for such behavior: a similar effect has been suggested as the cause of the apparent increase in k_{-CO} for $PhCH_2\dot{C}O$ with an increase in laser excitation power in normal liquids.[32] In fact we have demonstrated an 8-fold increase in k_{-CO} in 308-nm LFP of DBK in cyclohexane. k_{-CO} increased from 7.0×10^6 s^{-1} with 4 mJ/pulse excitation to 5.6×10^7 s^{-1} using 100 mJ/pulse. Nearly identical results to those presented in Figure 8 were obtained in SC ethane. Therefore there appears to be no special effect on the decarbonylation process of phenylacetyl radical due to SC solvent effects. This is reasonable since the time required for decarbonylation (step 4) is on the order of 100 ns while the solvent cage around the solute maintains its integrity for only a few nanoseconds, according to molecular dynamics simulations.[33]

Conclusions

LFP has been used to directly measure the rate constants of TTA of ^{3}BP in CO_2 and the free radical termination reaction of $Ph\dot{C}H_2$ in SC CO_2 and ethane. In each case the reactions are found to occur at the diffusion-controlled limit when the correct spin statistical factors are taken into account. The higher local density of solvent around the solute does not in any way impede the diffusion of ^{3}BP or the $Ph\dot{C}H_2$, as has been noted previously for pyrene[4] and nitroxide radical.[3] This is reasonable since the characteristic lifetime of the cluster, according to molecular dynamics calculations,[33] is on the order of a few nanoseconds, while the characteristic time for diffusion is much longer. Moreover, the solvent clustering does not in any way influence the encounter pair. For instance, the higher local density of solvent around the encounter pair does not increase the collision time or number of collisions sufficiently to overcome the required spin statistical factor for an encounter. This is consistent with the lifetime of the solvent cluster being significantly shorter than what one would anticipate being needed to overcome the spin

statistical factors. Therefore, based on the work presented here we conclude that clustering effects reported in the literature[3,4] that enhance reactivity and decrease deactivation processes may be specific to the chemical and physical processes involved.

The TTA reaction of ^{3}BP and the free radical termination of $PhC\dot{H}_2$ occur at the spin factor diffusion-control limit based on uniform distribution of the solute molecules in solution. Therefore, in these reactions there are no enhanced solute–solute interactions, in contrast to what has been suggested by theoretical calculations,[34] molecular dynamics simulations,[35] and some experimental investigations.[36,37] The calculations and simulations show a very large peak in the solute–solute radial distribution function, which indicates that the probability of finding one solute molecule in the vicinity of another is higher than if the solutes were uniformly distributed. In fact, the simulations for $1–2 \times 10^{-2}$ M solute in a Lennard-Jones supercritical fluid indicate the presence of up to one extra solute within four solute molecular diameters. Then it is reasonable to expect this higher local solute concentration to influence diffusion-controlled solute–solute reactions. However, this is not the case for the TTA reaction of ^{3}BP or the free radical termination of $PhC\dot{H}_2$. A possible explanation for the absence of solute–solute effects is that the concentration of ^{3}BP is very dilute (on the order of micromolar), such that even though benzophenone might not be uniformly distributed, the ^{3}BP is at infinite dilution. In fact, the simulations were performed at a much higher solute concentration than that used in either of these reactions. In the benzyl radical termination, significant energy is added to the dibenzyl ketone to cause the homolytic cleavage; thus it could be argued that this disrupts the equilibrium distribution of the species. Therefore, the absence of solute–solute effects in these reactions may be due to the specifics of the species involved. However, it is interesting to note that solute–solute effects were absent in the nitroxide free radical reaction[3] and the pyrene excimer formation,[4] as well.

These results illustrate that the solvent cluster around a solute in a supercritical fluid will affect chemical and physical processes only if the time scale of those processes are on the same order of magnitude as the time that the cluster maintains integrity and will be determined by the specifics of the processes. In addition, the TTA of ^{3}BP and the free radical termination of $PhC\dot{H}_2$ occurred at diffusion control (with spin statistical factors), showing no evidence of enhanced solute–solute interactions influencing reaction rates in supercritical fluids. Therefore, one should not overemphasize the importance of SC solvent cage effects or solute–solute interactions when considering reaction rates and mechanisms in SCFs.

Acknowledgment. We would like to thank Dr. Gordon Hug for access to his mixed-order kinetics program and for several helpful discussions. The work described herein was supported by the National Science Foundation; the donors of the Petroleum Research Fund, administered by the American Chemical Society; and the Office of Basic Energy Sciences of the U.S. Department of Energy. This is Contribution No. NDRL-3542 from the Notre Dame Radiation Laboratory.

References and Notes

(1) See contributions in the following: (a) *Supercritical Fluid Engineering Science: Fundamentals and Applications*; Kiran, E., Brennecke, J. F., Eds.; ACS Symposium Series 514; American Chemical Society: Washington, DC, 1993. (b) Eckert, C. A.; Knutson, B. L. *Fluid Phase Equilib.* in press. (c) *Supercritical Fluid Technology*; Bright, F. V., McNally, M. E. P., Eds.; ACS Symposium Series 488; American Chemical Society: Washington, DC, 1992. (d) *Supercritical Fluid Technology: Reviews in Modern Theory and Applications*; Bruno, T. J., Ely, J. F., Eds.; CRC Press: Boca Raton, FL, 1991. (e) *Supercritical Fluid Science and Technology*; Johnston, K. P., Penninger, J., Eds.; ACS Symposium Series 406; American Chemical Society: Washington, DC, 1989.

(2) (a) Sun, Y.-P.; Fox, M. A.; Johnston, K. P. *J. Am. Chem. Soc.* **1992**, *114*, 1187–1194. (b) Sun, Y.-P.; Bennett, G.; Johnston, K. P.; Fox, M. A. *J. Phys. Chem.* **1992**, *96*, 10001–10007. (c) Johnston, K. P.; Kim, S.; Combes, J. In ref 1e, pp 52–70. (d) Kim, S.; Johnston, K. P. *AIChE J.* **1987**, *33* (10), 1603–1611. (e) Kim, S.; Johnston, K. P. *Ind. Eng. Chem. Res.* **1987**, *26*, 1206–1214.

(3) Randolph, T. W.; Carlier, C. *J. Phys. Chem.* **1992**, *96*, 5146–5151.

(4) (a) Zagrobelny, J.; Betts, T. A.; Bright, F. V. *J. Am. Chem. Soc.* **1992**, *114*, 5249–5257. (b) Zagrobelny, J.; Bright, F. V. *J. Am. Chem. Soc.* **1992**, *114*, 7821–7826.

(5) O'Shea, K. E.; Combes, J. R.; Fox, M. A.; Johnston, K. P. *Photochem. Photobiol.* **1991**, *54*, 571–576.

(6) Chateauneuf, J. E.; Roberts, C. B.; Brennecke, J. F. In ref 1c, Chapter 9, pp 106–120.

(7) Roberts, C. B.; Chateauneuf, J. E.; Brennecke, J. F. *J. Am. Chem. Soc.* **1992**, *114*, 8455–8463.

(8) (a) Angus, S., Armstrong, B., de Reuck, K. M., Eds. *International Thermodynamic Tables of the Fluid State: Carbon Dioxide*; Pergamon Press: Oxford, 1976. (b) Younglove, B. A.; Ely, J. F. *J. Phys. Chem. Ref. Data* **1988**, *16* (4), 577.

(9) For a thorough review of spin statistical factors in diffusion-controlled reactions, see: Saltiel, J.; Atwater, V. W. *Adv. Photochem.* **1988**, *14*, 1–90.

(10) (a) Brown, R. E.; Singer, L. A.; Parks, J. H. *J. Am. Chem. Soc.* **1972**, *94*, 8584–8586. (b) Fang, T.-S.; Fukuda, R.; Brown, R. E.; Singer, L. A. *J. Phys. Chem.* **1978**, *82*, 246–248. (c) Yekta, A.; Turro, N. J. *Mol. Photochem.* **1972**, *3* (4), 307–322.

(11) Lehni, M.; Schuh, H.; Fisher, H. *Int. J. Chem. Kinet.* **1979**, *11*, 705–713.

(12) Carmichael, I.; Hug, G. L. *J. Phys. Chem. Ref. Data* **1986**, *15*, 54.

(13) Przybytek, J. T. *Solvent Guide*, 2nd ed.; Krieger, P. A., Ed.; Burdick & Jackson Laboratories, Inc.: Muskegon, MI, 1984; p 12.

(14) The mixed-order analysis is based on that previously described: Gorman, D. S.; Connolly, J. S. *Int. J. Chem. Kinet.* **1973**, *V*, 977–989.

(15) Iwasaki, H.; Takahashi, M. *J. Chem. Phys.* **1981**, *74*, 1930–1943.

(16) Kennedy, J. T.; Thodos, G. *AIChE J.* **1961**, *7*, 625–631. Also see: Reid, R. C.; Prausnitz, J. M.; Poling, B. E. *The Properties of Gases and Liquids*, 4th ed.; McGraw-Hill: New York, 1987; pp 424–426.

(17) Imotev, M. B.; Tsekhanskaya, Yu. V. *Russ. J. Phys. Chem.* **1964**, *38* (4), 485–487.

(18) For an excellent review of diffusion in supercritical fluids, see: Liong, K. K.; Wells, P. A.; Foster, N. R. *J. Supercrit. Fluids* **1991**, *4*, 91–108.

(19) Encinas, M. V.; Scaiano, J. C. *J. Am. Chem. Soc.* **1981**, *103*, 6393–6397.

(20) Godfrey, T. S.; Hilpern, J. W.; Porter, G. *Chem. Phys. Lett.* **1967**, *1*, 490–492.

(21) March, J. *Advanced Organic Chemistry*, 4th ed.; Wiley-Interscience: New York, 1992; p 191.

(22) Giering, L.; Berger, M.; Steel, C. *J. Am. Chem. Soc.* **1974**, *96*, 953–958.

(23) (a) Engel, P. S. *J. Am. Chem. Soc.* **1970**, *92*, 6074–6076. (b) Robbins, W. K.; Eastman, R. H. *J. Am. Chem. Soc.* **1970**, *92*, 6076–6077, 6077–6079.

(24) Porter, G.; Windsor, M. W. *Nature* **1957**, *180*, 187–188.

(25) Brocklehurst, B.; Porter, G.; Savadatti, M. I. *Trans. Faraday Soc.* **1964**, *60*, 2017–2021.

(26) Arbour, C.; Atkinson, G. H. *Chem. Phys. Lett.* **1989**, *159*, 520–525.

(27) Porter, G.; Wright, M. W. *Trans. Faraday Soc.* **1955**, *51*, 1469–1474.

(28) For reviews on solvent effects on electronic spectra, see: (a) Rao, C. N. R.; Singh, S.; Senthilnathan, V. P. *Chem. Soc. Rev.* **1976**, *5*, 297–316. (b) Nichol, M. F. *Appl. Spectrosc. Rev.* **1974**, *8*, 183–227. (c) Amos, A. T.; Burrows, B. L. In *Advances in Quantum Chemistry*; Löwdih, P.-O., Eds.; Academic Press: New York, 1973; pp 289–313.

(29) Claridge, R. F. C.; Fisher, H. *J. Phys. Chem.* **1983**, *87*, 1960–1967.

(30) Solvent effects on absolute intensities of electronic transitions are not as well understood as solvent-induced spectral shifts,[28] however, organic molecules often demonstrate an increase in absorption intensity in solution compared to the gas phase. Such effects have been discussed in terms of classical oscillator theory and changes in transition moments due to polarization of solutes by solvent.[28]

(31) (a) Lunazzi, L.; Ingold, K. U.; Scaiano, J. C. *J. Phys. Chem.* **1983**, *87*, 529–530. (b) Turro, N. J.; Gould, I. R.; Baretz, B. H. *J. Phys. Chem.* **1983**, *87*, 531–532.

(32) Gould, I. R.; Baretz, B. H.; Turro, N. J. *J. Phys. Chem.* **1987**, *91*, 925–929.

(33) Petsche, I. B.; Debeneditti, P. G. *J. Chem. Phys.* **1989**, *91*, 7075–7084.

(34) Wu, R.-S.; Lee, L. L.; Cochran, H. D. *Ind. Eng. Chem. Res.* **1990**, *29*, 977–988.

(35) Chialvo, A. A.; Debenedetti, P. G. *Ind. Eng. Chem. Res.* **1992**, *31*, 1391–1397.

(36) Hrnjez, B. J.; Mehta, A. S.; Fox, M. A.; Johnston, K. P. *J. Am. Chem. Soc.* **1989**, *111*, 2662–2666.

(37) Randolph, T. W.; Clark, D. S.; Blanch, H. W.; Prausnitz, J. M. *Science* **1988**, *239*, 387.